In vivo confirmation of hydration-induced changes in human-skin thickness, roughness and interaction with the environment

Running title: Hydration-induced changes in human skin

Running Authors: Dąbrowska et al.

Agnieszka K. Dąbrowska[a)]

Empa, Swiss Federal Laboratories for Materials Science and Technology, Laboratory for Protection and Physiology, CH-9014, St. Gallen, Switzerland
ETH Zürich, Department of Materials, Laboratory for Surface Science and Technology, CH-8093 Zürich Switzerland

Christian Adlhart

Zurich University of Applied Sciences, ZHAW, Institute of Chemistry and Biotechnology, CH-8820, Wädenswil, Switzerland

Fabrizio Spano

Empa, Swiss Federal Laboratories for Materials Science and Technology, Laboratory for Protection and Physiology, CH-9014, St. Gallen, Switzerland

Gelu-Marius Rotaru

Empa, Swiss Federal Laboratories for Materials Science and Technology, Laboratory for Protection and Physiology, CH-9014, St. Gallen, Switzerland

Empa, Swiss Federal Laboratories for Materials Science and Technology, Center for X-ray Analytics, CH-8600 Dübendorf, Switzerland

Siegfried Derler

Empa, Swiss Federal Laboratories for Materials Science and Technology, Laboratory for Protection and Physiology, CH-9014, St. Gallen, Switzerland

Lina Zhai

Empa, Swiss Federal Laboratories for Materials Science and Technology, Laboratory for Protection and Physiology, CH-9014, St. Gallen, Switzerland

Donghua University, Fashion Institute, Protective Clothing Research Center, 200051, Shanghai, China

Nicholas D. Spencer

ETH Zürich, Department of Materials, Laboratory for Surface Science and Technology, CH-8093 Zürich Switzerland

René M.Rossi

Empa, Swiss Federal Laboratories for Materials Science and Technology, Laboratory for Protection and Physiology, CH-9014, St. Gallen, Switzerland

[a]Electronic mail: agnieszka.dabrowska@empa.ch

Skin properties, structure and performance can be influenced by many internal and external factors, such as age, gender, lifestyle, skin diseases and a hydration level that can vary in relation to the environment.

2

The aim of this work was to demonstrate the multifaceted influence of water on human skin through a combination of *in vivo* confocal Raman spectroscopy and images of volar-forearm skin captured with laser scanning confocal microscopy. By means of this pilot study, we have both qualitatively and quantitatively studied the influence of changing the depth-dependent hydration level of the *stratum corneum* (SC) on the real contact area, surface roughness and the dimensions of the primary lines and presented a new method for characterising the contact area for different states of the skin.

The hydration level of the skin and the thickness of the SC increased significantly due to uptake of moisture derived from liquid water or, to a much lesser extent, from humidity present in the environment. Hydrated skin was smoother and exhibited higher real contact area values. The highest rates of water uptake were observed for the upper few μm of skin and for short exposure times.

I. INTRODUCTION

Skin is our protective armor in everyday life [1] and our primary interface with the environment. It has an area of some 2m^2, and is thus the largest single organ in the human body. Human skin is a multilayer structure, consisting of the *epidermis*, being the outer layer of the skin, mostly exposed to the external factors, *dermis*, responsible for, *inter alia*, flexibility and durability of the skin and subcutaneous tissue, acting as additional insulation and mechanical protection [2-4]. One of the main functions of skin is to protect the body from external factors, such as mechanical injuries, extremes of temperature and radiation, as well as the transport of various substances [5, 6]. The barrier function of skin is

mostly provided by the *stratum corneum* ("horny layer", SC) [7-9]. This thin layer, reaching a thickness of 15-20 μm at the volar forearm, is the most external of the sublayers of *epidermis* [1,7]. Keratinocytes, comprising about 85% of the *epidermis*, migrate through the sublayers of the *epidermis*, gradually transforming to horny cells by changing their size, shape, composition and losing their nuclei. The SC consists of non-nucleated and flat cells named corneocytes[10,11]. According to the "brick and mortar" model, corneocytes are described as bricks surrounded by lipid bi-layers as the mortar [8]. The hydration level of the SC can vary depending on environmental conditions, as corneocytes can take up water until the hydration level of the SC is in equilibrium with the environment [12]. The hydration level of the SC is responsible for the physiology and homeostasis of the skin [13]. Examples of the importance of hydration on the functions and properties of the skin are its influence on the mechanical toughness of skin, its barrier functions and the regulation of enzyme activity [7,14-16]. As suggested by Egawa, daily routines can lead to visible changes in the skin [17]. Even a very short exposure to water, such as washing hands for 2 minutes, is enough to hydrate the SC *disjunctum* while a bath can contribute to changes in the SC *conjunctum*, and thus the influence of the environment on the properties of the skin are essential factors to be taken into account when studying skin-materials interactions [18,19]. Moreover, seasonal changes in humidity are an important factor influencing the skin [20].

There is a variety of techniques that allow both *in vivo* and *in vitro* determination of the hydration level of skin, based on different principles, including chemical analysis and electrical methods [21-25]. For the purposes of this paper, we have chosen confocal Raman

spectroscopy as a non-invasive, depth-resolved method that provides quantitative information concerning the skin's hydration level.

The results extracted from confocal Raman spectroscopy provide information on hydration and its variation with depth, the SC thickness and also, in combination with information on the real contact area of skin with the Raman instrument, inferences about the interaction of skin with other objects [9, 15, 26-30].

Given that skin is able to take up water, it is reasonable to assume that water should also change its morphology and surface properties. In order to analyze these changes over time, we have employed 3D laser scanning microscopy, which allowed us to observe the surface of a skin replica under high magnification and provided 3-D information [31-33].

In this paper, we present a pilot study focused on global changes in appearance and properties of human skin caused by exposure to water or humid conditions. In order to investigate the multifaceted response of skin to water we have examined the hydration level of the superficial stratum corneum (SSC), being the surface of skin, depth profiles of skin before and after exposure to external sources of water, the skin's water uptake abilities, the SC thickness, the real contact area against smooth CaF_2, the skin's surface roughness, and the evolution of the dimensions of the primary lines.

II. EXPERIMENTAL SETUP AND METHODOLOGY

A. Instrumentation

1. Confocal Raman Spectroscopy

The hydration level of skin was determined from *in vivo* Raman spectra that were acquired using an inverted confocal Raman spectrometer equipped with a 60x oil

immersion objective, Skin Composition Analyzer (SCA), model 3510 (RiverD, Rotterdam, the Netherlands). Depth profiles were measured in 2 μm steps, from the surface of the skin to a depth of 60 μm. Laser excitation with a wavelength of 671 nm (laser power 19.5 ± 1.8 mW) was used for 1 s in order to obtain spectra in the region of 2550-4000 cm^{-1}, providing information about the amount of water and proteins in the skin [16, 34, 35]. The *z*-resolution of the optical setup was determined to be 4.7 µm by placing a water droplet on the CaF_2 window of the inverted microscope and fitting the slope of the Raman signal at the CaF_2/water interface with a Lorentz function, taking the full width at half maximum. To account for the known discrepancy between true confocal depth and mechanical displacement of the optical table [36], all depth profiles were corrected with the depth-correction factor f_{depth} = 1.06. f_{depth} was determined by comparing the confocal thickness of a NIST polystyrene standard film with its true thickness. Therefore, the film was placed onto the CaF_2 window with an additional water contact layer of approx. 5 µm and the Raman signal of polystyrene between 3040 and 3076 cm-1 was followed in steps of 0.5 µm. The true thickness of the polystyrene film was determined to be 52.7 µm as calculated from the infrared transmission interference pattern in the 3200 to 3600 cm^{-1} wavenumber region (refractive index $n_{polystyrene}$ = 1.59).

2. *3D Laser Scanning Confocal Microscopy*

The surface morphology of polyvinylsiloxane (Profil novo light type 3, Heraeus Kulzer GmbH, Hanau, Germany) skin replicas was observed by means of a 3D Laser Scanning Confocal Microscope, model VK-X250 (Keyence, Osaka, Japan), using a violet laser with a wavelength of 408 nm (maximum laser power: 0.95 mW).

B.   Measurements

The single-person pilot study was performed on a healthy, left-handed Caucasian woman aged 26 with a BMI of 21. For at least 48 hours before the measurements, the skin was not treated with moisturizers and heavy exercises were avoided. All measurements were performed on the left arm. For simplicity, the skin before water/humidity exposure is termed "dry", whereas the skin exposed to an external source of water is termed "hydrated". After exposure to water/humidity, the forearm was immediately placed on the CaF_2 acquisition window of the Raman instrument and maintained in this position throughout the entire measurement. After each depth profile, the lateral position of the laser was changed between 0.2 and 2.0 mm and another depth profile was collected. The measurements, consisting of 10 depth profiles collected at 10 different positions on the volar forearm, were repeated three times for each exposure time/set of conditions.

1.   Influence of water on skin hydration

Hydration levels of skin under atmospheric conditions were measured at four different points that were equally distributed along a line from about 7 cm from the wrist up to the elbow (Figure 1a). Then the defined measuring points were exposed to water using patch-test chambers (Van der Bend, Brielle, the Netherlands) filled with 20 µl of distilled water. Exposure time was varied from 2 to 60 minutes. After unsticking the patch, excess water was removed with a paper towel.

2. Influence of water vapor on skin hydration

Hydration levels of skin under atmospheric conditions as well as after exposure to air at a defined humidity were measured midway between the wrist and the elbow. To expose skin to an atmosphere at a specified humidity, the left arm was placed in a purpose-built PMMA humidity chamber with the dimensions of 60 x 50 x 30 cm for one hour (Figure 1b). Saturated NaCl solution or a travel air humidifier, both assisted by a fan to homogenize the air inside the chamber, were used in order to obtain a relative humidity of 70 or 90%, respectively [37, 38].

3. Surface morphology

Polyvinylsiloxane replicas of the skin taken before and after 2-60 minutes of exposure to water (according to the same procedures as explained above) were prepared in triplicate. The change in surface morphology due to exposure to water was investigated by means of a 3D laser scanning confocal microscope. Each replica was analyzed in three different spots using the 20 x objective lens.

C. Data processing

1. Hydration level

Hydration levels of skin were automatically determined from the Raman spectra using Skin Tools 2.0 software (RiverD, Rotterdam, the Netherlands), where the water content is calculated relative to keratin, based on the integrals of OH-vibration signals (W) in the

range of 3350 to 3550 cm^{-1} and the integrals of the relevant CH-vibration signals (2910-2966 cm^{-1}), P) [16, 21, 34, 39], using the relation

$$hydration\ level\ (\%) = \frac{W/P}{W/P+R} * 100\%$$

according to Caspers *et al* [21], where $R = 2$ is a proportionality constant that was obtained by calibrating against protein solutions. To determine the integrals W and P, Raman spectra were baseline corrected with a first-order polynomial fitted through the spectral regions 2580 to 2620 and 3780 to 3820 cm^{-1}, see also Figure 2.

Both the absolute hydration level and the water uptake, understood as the difference between the hydration level before and after exposure to water, were taken into consideration in further investigations.

Biexponential fitting was applied to the data of time-dependent change in hydration level of *superficial stratum corneum* according to

$$hl(t) = hl_0 + hf_A \times [1 - e^{-k_A \times t}] + hf_B \times [1 - e^{-k_B \times t}]$$

where hl(t) and hl_0 are the respective hydration levels at time t and at $t = 0$ min. The variables hf and k are the hydration factor in % and the hydration rate coefficient in min^{-1} for the two exponential functions A and B, see also Figure 3.

2.   *Contact area*

We propose a new non-invasive in vivo method to measure the influence of hydration on the contact area between skin and other objects. For each spectrum, an image of the contact between the skin and the CaF$_2$ acquisition window of the SCA was taken. Based

on the images corresponding to each spectrum, the contact area could be calculated by means of CorelDRAW X6 software, supported with the Getarea macro.

3. Thickness of the stratum corneum

As proposed by Crowther, the thickness of the SC can be determined from each water profile by fitting with a Weibull curve [16, 34, 40]. This was performed with Matlab (The Mathworks, Natick, MA, U.S.A).

4. Surface morphology

Surface-roughness parameters: Sa, Sz, and the characteristic dimension of the profiles were extracted with VK-H1XME: VK-X AI-Analyzer Software, each measurement being the average of three profiles with the interval of 20 μm of replicas. Each image was inverted and artefacts as well as characteristic features, such as sweat glands, hair follicles etc. were not considered in further data processing.

III. RESULTS

A. Raman spectra of the stratum corneum and viable epidermis before and after exposure to water

Raman spectra of skin show characteristic features depending on the sampling depth and the preconditioning of the skin (Figure 2). For dry skin the Raman spectrum captured at the SSC (0 μm depth) level shows strong CH-vibration signals that are characteristic of

proteins (2930 cm^{-1}) and lipids (2850 and 2880 cm^{-1}), as well as weak OH-vibration signals (3350 to 3550 cm^{-1}) characteristic of water (Figure 2a). This is in contrast to the spectrum captured in the VE (40 µm depth) (Figure 2b), where the strong lipid signals are absent, and the OH- signals are stronger, corresponding to a higher water content. After 1h exposure to water, the spectrum captured at the SSC level shows a strong water peak (Figure 2a) while no such significant change was observed in the VE-level spectrum (Figure 2b).

B. *Environmentally dependent changes in the structure and properties of human skin*

1. *Hydration level of the stratum corneum*

Figure 3 shows the influence of the environment on the hydration level at the surface of the skin, at 0 µm depth (SSC). It can be clearly seen that water exposure influenced the hydration level of the SSC to a far higher extent than was observed for relative humidity up to 90%. The level of hydration gradually increased from 26.2 ± 3.4% to 60.2 ±7.0% after 60 minutes of water exposure. The extent of the forced hydration was significant, especially for short exposure time (up to 5 minutes).

Increase in relative humidity (RH) from 40% to 90% contributed towards an increase in the hydration level of the SSC from 24.7 ± 3.5% to 27.6 ± 3.8% after 60 minutes. In comparison, a significantly higher hydration level (35.2 ± 5.0 %) was observed after just 2 minutes exposure to liquid water.

Consistent with the abovementioned phenomenon, it was also clear from the depth profiles of water content (Figure 4a) that the hydration level in the SSC increased most significantly after exposure to water. In addition to the results presented on the Figure 3, the depth profiles show that the largest change in hydration level caused by external factors could be observed within the first 10 μm. The hydration level of dry skin varied with depth from 26.2 ± 3.4% in the SSC to 70.3 ± 2.9% in the VE at a depth of 50 μm. Depth profiles before and after exposure to the external source of water coincide for deeper layers of the skin. In order to show this effect even more clearly, the hydration level measured at different depths of the skin from 0 to 10 μm were plotted as a function of the exposure time to water (Figure 4b). As presented in the graph, the influence of the exposure time to water on the hydration level was more marked for the (initially drier) outer layers of the skin. Water uptake, being the difference between the hydration level of the skin before and after water exposure for different depths of the skin, is presented on Figure 5. Confirming the effect visible on Figure 4, Figure 5 presents the uptake of water at different depths of the skin when the skin was exposed to water for 2, 30 and 60 minutes. It is clearly visible that the deeper the layer of skin that was investigated, the lower was the uptake of water. The hydration rate also decreased with exposure time. Considering the surface of the skin, the uptake of water after 2 minutes of exposure was 9.03 ± 6.03 %, changing to 26.53 ± 7.47 % after 30 minutes and 34.02 ± 8.95 % after 60 minutes.

2.   The evolution of contact area

The real contact area, which corresponds to direct contact between skin and the CaF_2 acquisition window, can be recognized as dark areas in Figures 6a-d, which were captured within the first few seconds after the forearm was placed on the CaF_2 window. The rapid acquisition was necessary in order to avoid the influence of sweating and relaxation process and to show the clear influence of the external source of water on the contact area. Apparent contact area is defined as the area of the apparent contact between the skin and the CaF_2 window, which itself had an area of 70 734 μm^2.

From the very low real contact area values, it is clear that dry skin has little direct contact area with the CaF_2 window values (Figure 6a). This is due to its roughness and limited elasticity. After only 2 minutes exposure to water there was a significant increase in real contact area (Figure 6b). Longer exposures, such as 30 (Figure 6c) or 60 minutes (Figure 6d) did not lead to a significantly greater real contact area value.

Real/apparent contact area ratio for dry skin (hydration level: 26.2 ± 3.4%, as shown on Figure 2) had a value in the range of 36% (Figure 7a-b). Once the skin was exposed to water, the contact area significantly increased and real/apparent contact area ratio (hydration level 35.2 ± 5.0 %) reached 73% after 2 minutes exposure. Values of real contact area and real/apparent contact area ratio for skin exposed to water for 2-60 minutes were comparable.

In agreement with other analyses, the influence of humidity on the contact area was lower than it was measured for water. Real/apparent contact area ratio gradually increased from 35% for 40% RH to 48% for 90% RH.

3.   Thickness of the stratum corneum

As presented above, hydration measurements showed that human skin absorbs water from the environment. To confirm this phenomenon, measurements of the change in structure and morphology of human skin were performed.

Figure 8 presents the influence of water absorption on the thickness of the SC. When the skin was exposed to water, the thickness of the SC, determined based on the Raman spectra, increased linearly with increasing exposure time. The SC thickness increased from 17.5 ± 2.5 µm measured for skin before water exposure to 21.2 ± 3.0 µm after 60 minutes exposure to water. Exposure to humidity influenced the SC thickness to a smaller extent, causing an increase from 17.2 ± 2.0 µm for 40% RH to 18.5 ± 2.4 µm measured for the skin exposed to 90% RH for 60 minutes.

4.   Morphology of the skin

Figure 9 presents the surface roughness values; Sa (Figure 9e) and Sz (Figure 9f) as well as two- and three-dimensional micrographs of skin replicas of the volar forearm before (Figure 9a, c) and after 60 minutes exposure to water (Figure 9b, d). It can be observed that water changed the appearance of human skin, making it smoother. The Sa parameter decreased from 6.7 ± 0.7 µm measured for dry skin to 4.7 ± 0.5 µm measured after 60

minutes water exposure, due to the smoothening effect water uptake. Similarly, the value of the Sz parameter dropped from 84.3 ± 24.1 μm before to 53.6 ± 9.9 μm after exposure to water.

From the cross-section of the 3D microscopic pictures, surface profiles of dry (Figure 10a) and wet (Figure 10b) skin were extracted, in order to investigate the influence of exposure to water on the dimension of the clefts present on the skin. The average width of the primary lines decreased from 112.6 ± 30.7 μm before to 57.7 ± 16.0 μm after 60 minutes water exposure (Figure 10c). The depth of the primary lines also decreased, reducing from 44.5 ± 9.8 μm for dry skin to 20.5 ± 10.2 μm for skin exposed to water (Figure 10d).

IV. DISCUSSION

In the present study we were able to demonstrate how hydration conditions influence human skin on several levels. Under dry conditions, human skin can be considered as a rough material [1]. Dry SC is characterized by high values of Young's modulus, reaching into the GPa range [41-44]. Therefore, as a rough and not easily deformable material, characterized by wide and deep primary lines [44], human skin in a dry state shows limited real contact area with the CaF_2 window. The hydration level of dry skin increased with the depth of the measurement, exhibiting the lowest value for the SC, consisting of dead and shriveled corneocytes [5] and the highest value for VE [16, 35, 40, 45]. The natural variation of the water content at different depths of the skin is the explanation for a clear difference in the ratio between protein and water peaks in Raman spectra for the SC and VE of the dry skin.

The hydration state has a major influence on the performance of the skin. As can be seen in the Raman spectra, when the skin was exposed to water for 60 minutes, the ratio between the protein and water peaks for the SSC changed drastically due to water uptake. However, the exposure to water did not influence the VE [35]. Depth profiles also confirmed that water can only influence the surface of the skin and showed that, below a certain depth, there was no difference between dry and hydrated skin. This behaviour can be explained by the barrier function of the SC, as the threshold depth corresponds to the location of the lower SC, known to act as a barrier layer for water [46-49]. Another threshold can be observed, suggesting that the skin was more accessible to penetration of water, and that it occurred faster at depths of the first few μm of the SC. The time dependent change of the hydration level of the SSC (Figure 3) fits well to a biexponential model with a fast and slow hydration rate coefficient $k_A = 0.31$ min^{-1} and $k_B = 0.52*10^{-3}$ min^{-1}. This could indicate at least two different water diffusion mechanisms as expressed in the literature by multi-layer or multi-compartment skin models and the finding of true formation of water pools within the SC [50-52]. This observation is consistent with a statement by Loth, that the transport of water within the SC *disjunctum* takes place through spreading into the intercellular space due to the capillary forces, whereas the much slower and less straightforward water transport within the SC *conjunctum* is based only upon diffusion [18, 53-55]. This also explains the observation that the closer to the surface of the skin, the faster and more significant is the water uptake as well as the fact that even a short exposure to water (2 minutes) caused appreciable changes in the SSC.

As the SC becomes hydrated, it is no longer stiff and rough. Due to the plasticizing effect of water, the Young's modulus of the SC may decrease by as much as three orders of

magnitude [42, 44]. The dimensions of the primary lines decrease, making the surface of the skin smoother. Softer and smoother skin results in a significantly higher real contact area with the CaF_2 window. The uptake of water by corneocytes not only makes the main furrows shallower, but also leads to an increasing thickness of the SC [16, 35]. Water diffusion requires space and therefore leads to physical expansion, i.e. swelling [51, 52]. For all investigated parameters, an increase in relative humidity had a minor influence on the skin compared to direct contact with water. Skin hydrated through the exposure to humid conditions followed the same tendencies as the skin hydrated through direct exposure to water, but to a much lesser extent. In the case of our experiments, humid conditions can be compared with the amount of water in the air equal to 13,6 g/m^3 for the RH=70% and 19,6 g/m^3 for the RH=90% [56-58].

The observed effects caused by water on the skin are summarized in Figure 11.

V. CONCLUSIONS

In conclusion, although still consisting of the same cells and chemical components, hydrated skin can be perceived as a material with significantly different properties than skin in its usual dry state.

Our study shows that as a result of exposure to water, corneocytes take up the liquid, resulting not only in increased hydration on the SC, but also, due to swelling, in an increased SC thickness and a smoother surface. Moreover, plasticized SC exhibits a lower modulus, i.e. is more easily deformable, leading to a higher real contact area with the CaF_2 window and presumably other objects. This will clearly have tribological consequences.

17

Improved understanding of the influence of environmental conditions on the properties of human skin is important for various research areas. Barrier function of human skin is the focus of research useful for the drug delivery [59]. It was proven that hydration of the skin (and, consequently, environmental conditions) has a major impact on dermatological issues. Proper hydration is a requirement for the flawless wound healing process [60]. Various skin diseases are caused by skin dryness. Dermatological treatment of, example giving, Xerosis cutis or eczema, could be supported with monitoring and modification of the hydration level of skin [61]. Hydration of skin plays a key role also in ageing prevention [62]. Presented knowledge can be also useful for developing skin models or understanding skin-friction mechanisms, as skin friction is directly related to the skin hydration and environmental conditions and, as a consequence, skin roughness and real contact area with counter surfaces [26]. This could also contribute in the prevention of the decubitus ulcers, as the creation of ulcers depends on the friction between skin and the bedsheet [63].

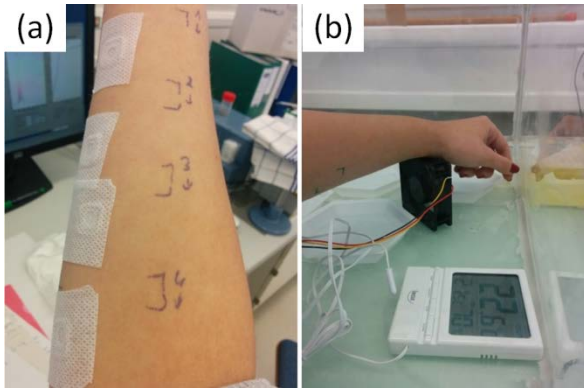## ACKNOWLEDGMENTS

LIST OF FIGURES

Figure 1. (a) Forearm exposed to water with the use of patch test chambers. (b) Forearm inside the humidity box.
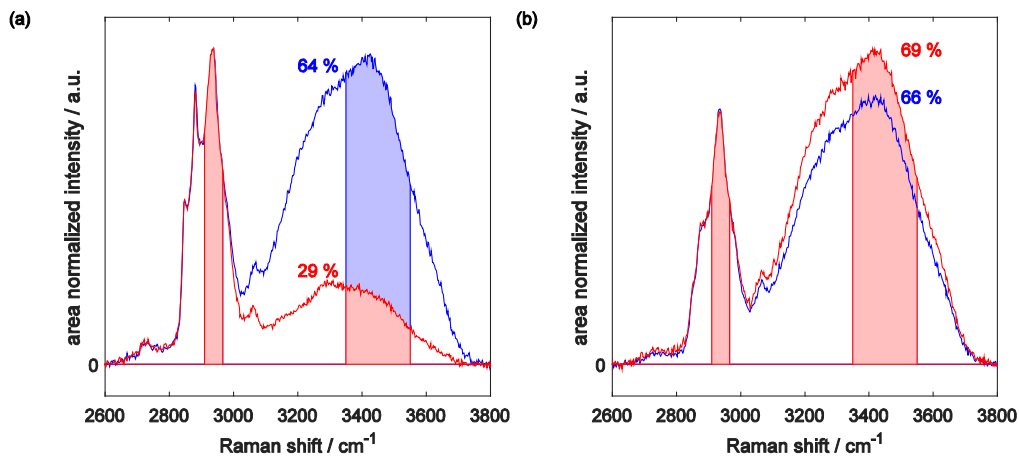

Figure 2. Typical base line corrected Raman spectra and hydration levels of the superficial stratum corneum at 0 µm (a) and of the viable epidermis at 40 µm (b) captured before (dry, red) and after 1 h exposure to water (wet, blue). Hydration levels were determined based on the ratio of protein and water vibrations (shaded areas). The difference of 3 % in (b) reflects the uncertainty of skin hydration due to local variation of the hydration level.
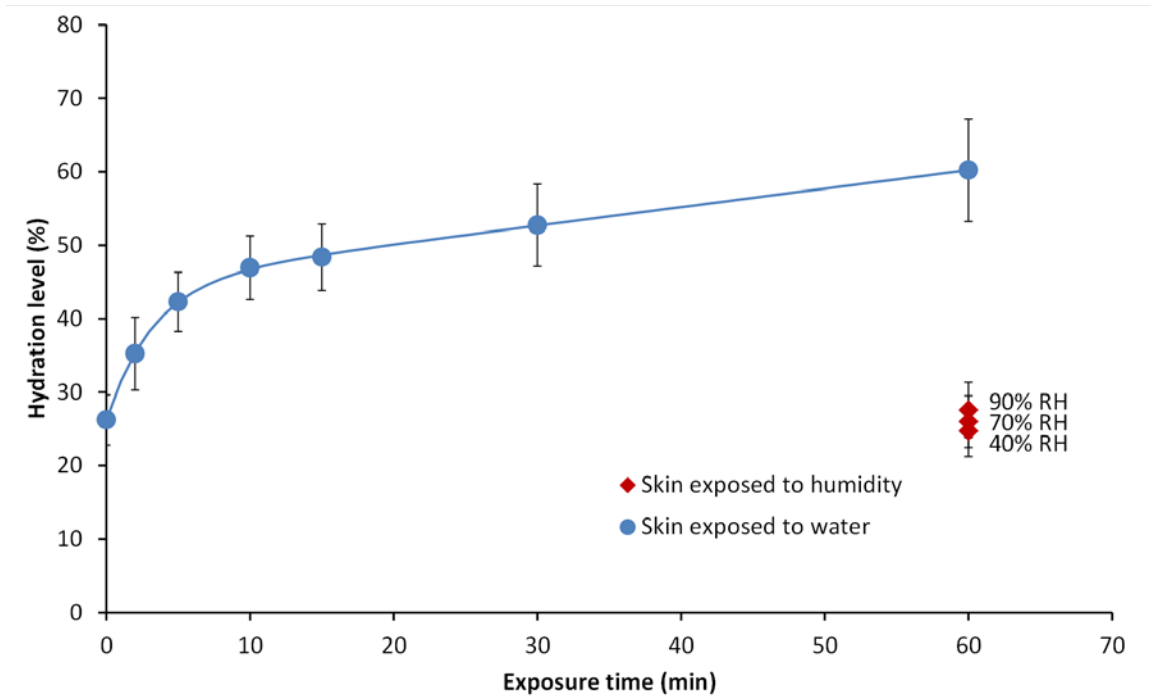
Figure 3. Change of hydration level of the superficial *stratum corneum* (SSC) caused by the water and humidity exposure. The straight line shows the biexponential fit with $hl_0 = 26.2$ %, the hydration factors $hf_A = 18.8$ % and $hf_B = 494$ %, and the fast and slow hydration rate coefficients $k_A = 0.31$ min^{-1} and $k_B = 0.52*10^{-3}$ min^{-1}.
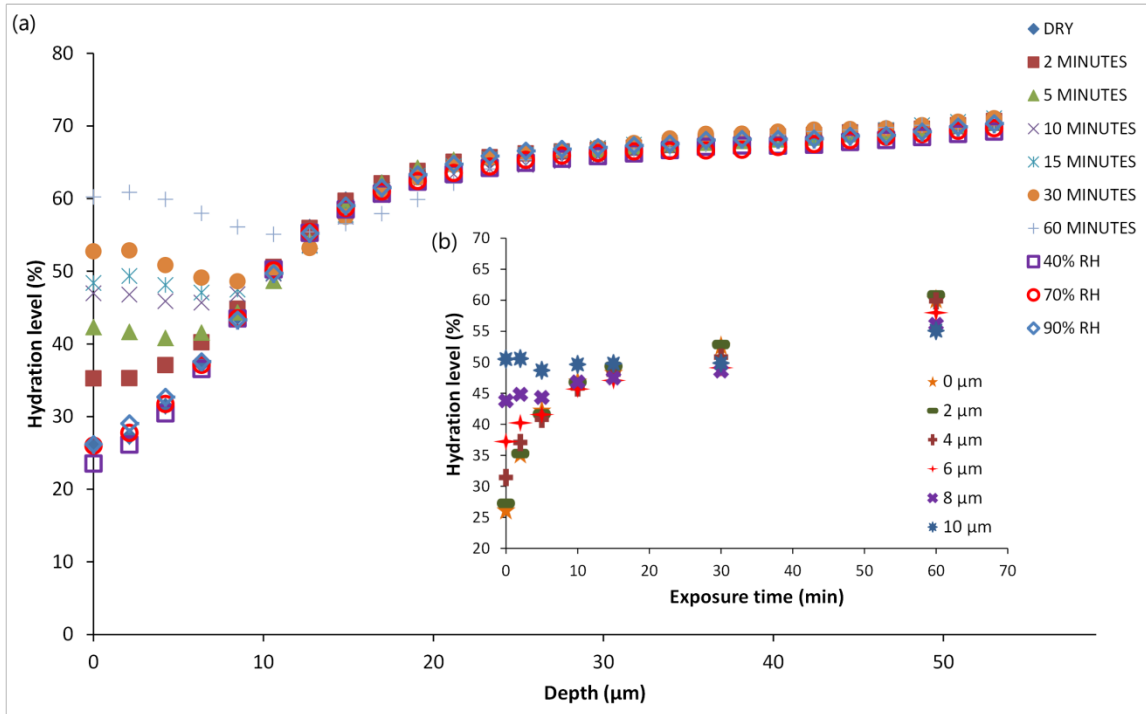
Figure 4. (a) Change of the depth profiles of water content in the SSC caused by water and humidity exposure. (b) Inset: Time-dependent change in the hydration level at depths up to 10 μm caused by water exposure.
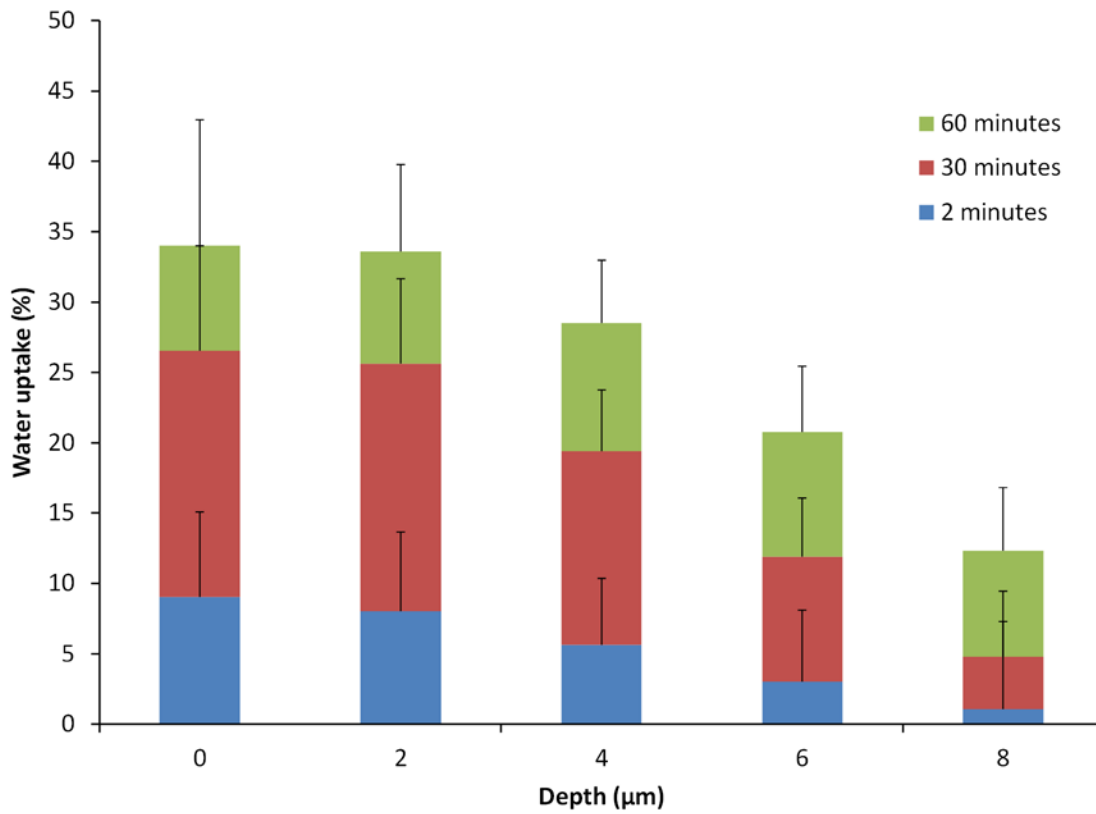
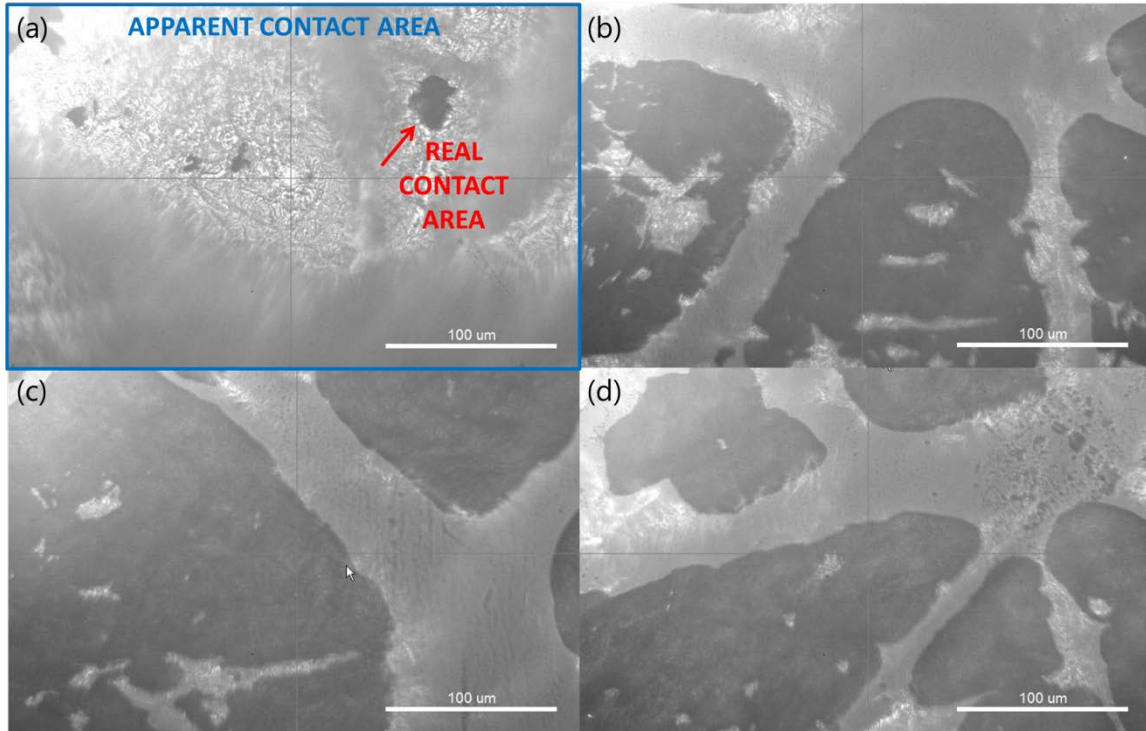Figure 5. Total uptake of water at different depths of the skin after different times of water exposure.

Figure 6. Evolution of the skin/CaF$_2$ acquisition window contact area before (a) and after 2 (b), 30 (c) and 60 (d) minutes of water exposure.
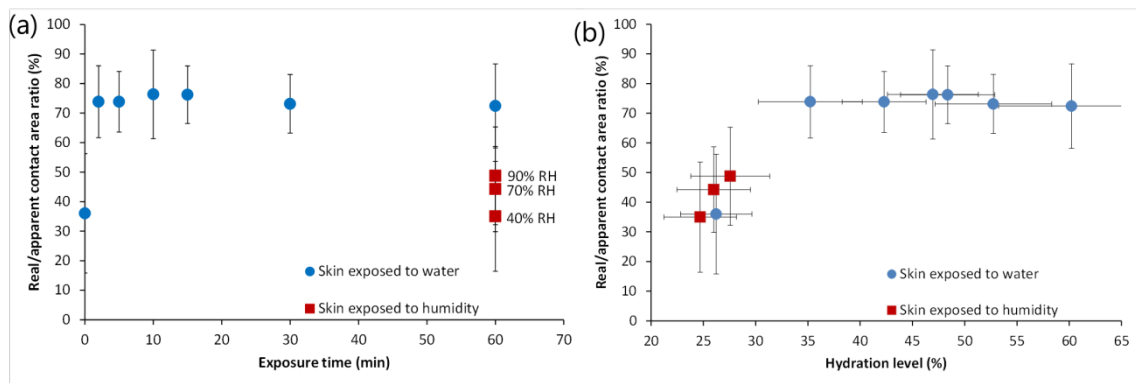

Figure 7. Change in the real/apparent contact area ratio caused by the water and humidity exposure (a). real/apparent contact area ratio as a function of the hydration level of the SSC (b).
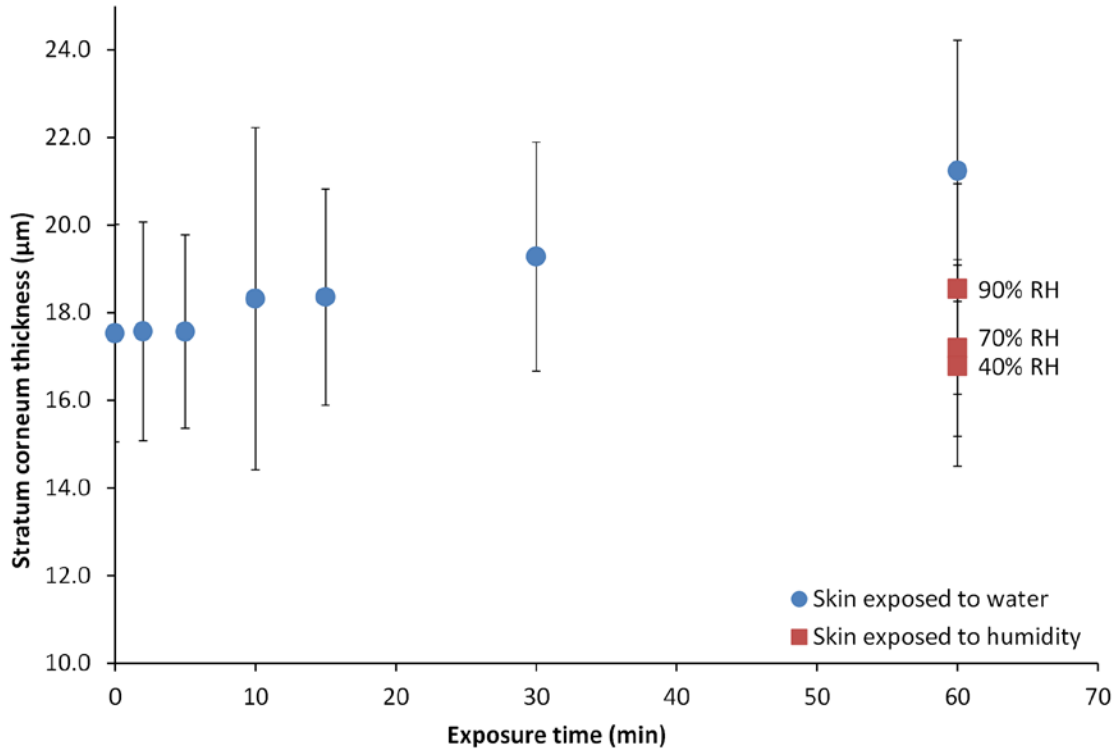
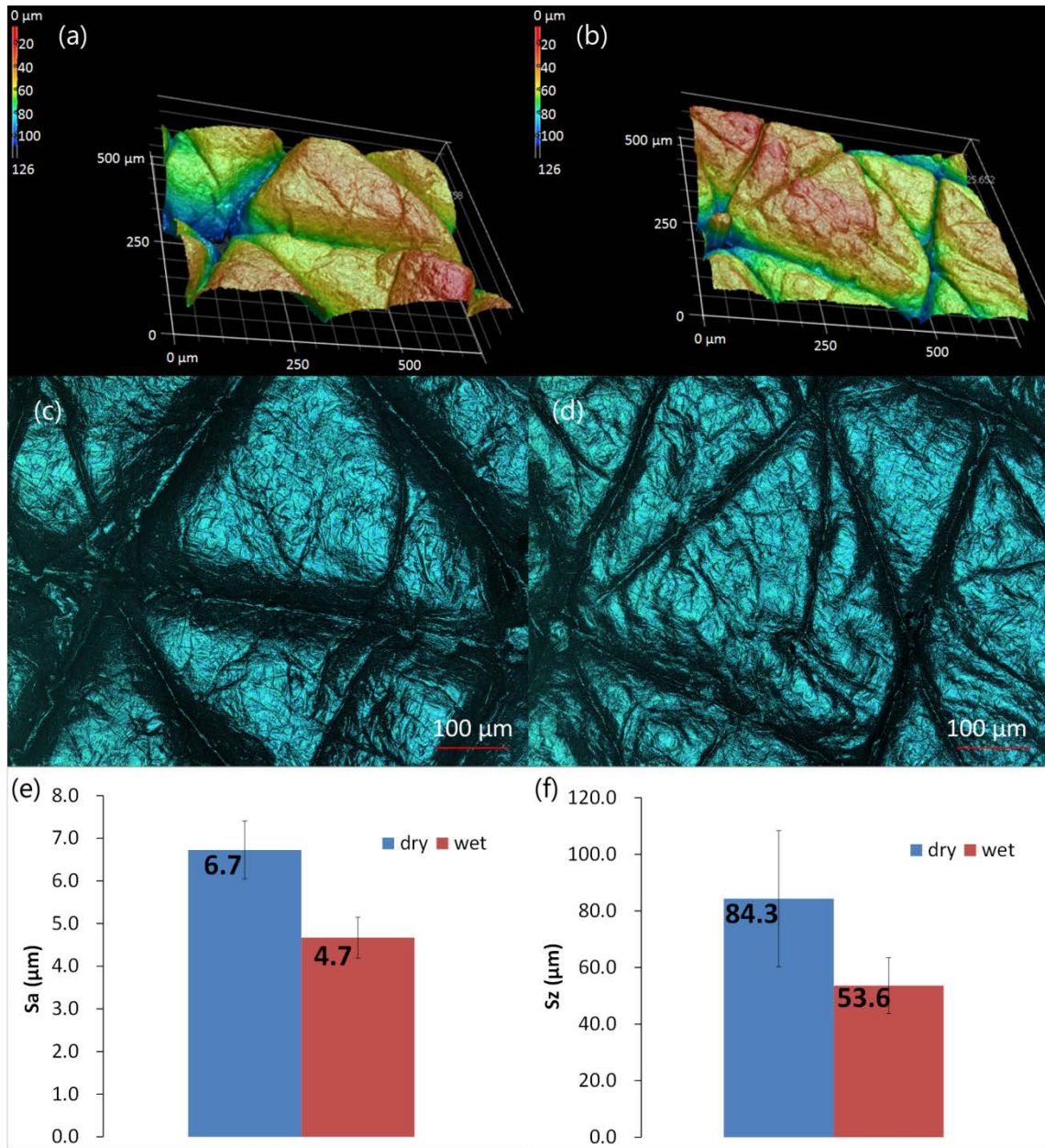Figure 8. SC thickness upon water and humidity exposure.

Figure 9. Appearance of human skin before (a: 3D topographical view, c: 2D topographical view) and after 60 minutes exposure to water (b: 3D topographical view, d: 2D topographical view). Surface roughness: Sa (e) and Sz (f) of human skin before (dry) and after 60 minutes water exposure (wet).
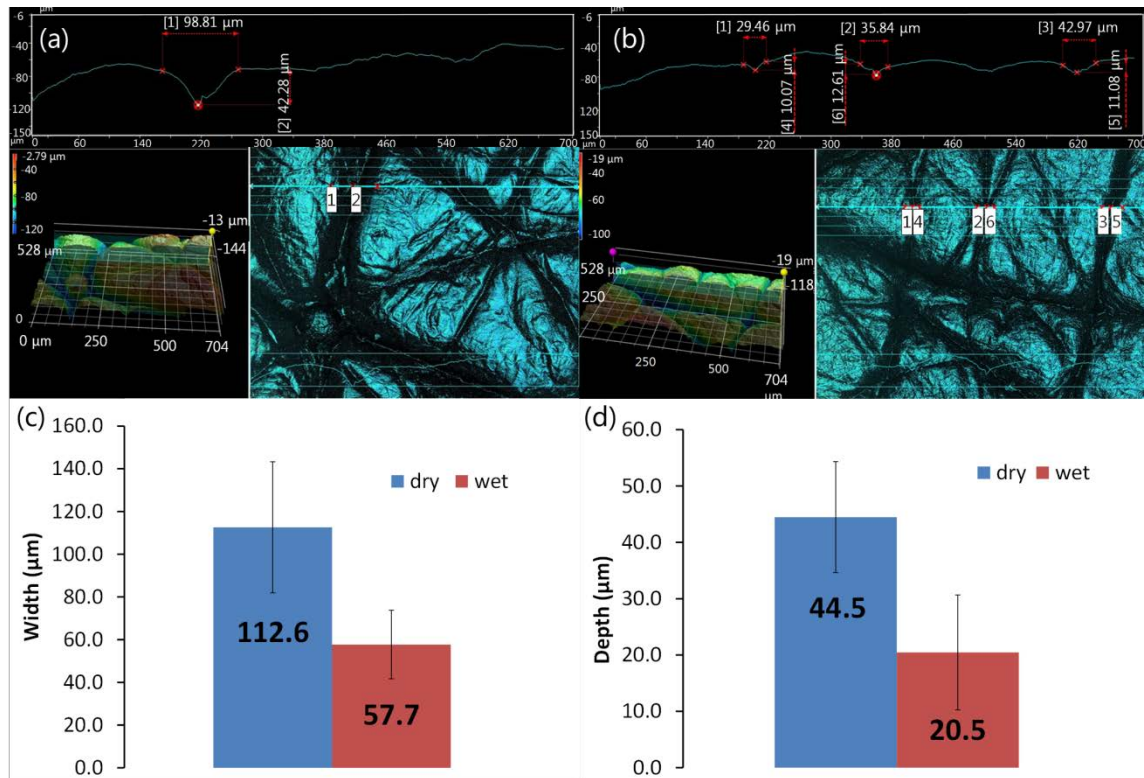
Figure 10. Surface profiles extraction from the 3D cross-section of the dry (a) and wet (b) skin replica. Width (c) and depth (d) of the primary lines before (dry) and after 60 minutes water exposure (wet).

Figure 11. The summary of observed changes in the structure and properties of skin caused by 60-minutes exposure to water.

1.   S. Derler and L. C. Gerhardt, Tribol Lett **45** (1), 1 (2012).

2.   W. James, T. Berger and D. Elston, Andrews' Diseases of the Skin Clinical Dermatology, 10th Edition. Phildelphia: Saunder Elsevier **12** (2006).

3.   J. G. Marks and J. J. Miller, *Lookingbill and Marks' principles of dermatology.* (Elsevier Health Sciences, 2013).

4.   J. Welzel, C. Reinhardt, E. Lankenau, C. Winter and H. Wolff, Brit J Dermatol **150** (2), 220 (2004).

5.   A. K. Dąbrowska, G. M. Rotaru, S. Derler, F. Spano, M. Camenzind, S. Annaheim, R. Stämpfli, M. Schmid and R. M. Rossi, Skin Research and Technology, n/a (2015).

6.   P. Koepke, M. Hess, S. Bretl and M. Seefeldner, presented at the CURRENT PROBLEMS IN ATMOSPHERIC RADIATION (IRS 2008): Proceedings of the International Radiation Symposium (IRC/IAMAS), 2009 (unpublished).

7.   P. J. Caspers, G. W. Lucassen, H. A. Bruining and G. J. Puppels, J Raman Spectrosc **31** (8-9), 813 (2000).

8.   P. M. Elias, J Invest Dermatol **80** (1983).

9.   F. D. Fleischli, S. Mathes and C. Adlhart, Vib Spectrosc **68**, 29 (2013).

10.   P. Elsner, in *Textiles and the Skin* (Karger Publishers, 2004), Vol. 31, pp. 24.

11.   H. Beele, The International journal of artificial organs **25** (3), 163 (2002).

12.   C. L. Silva, D. Topgaard, V. Kocherbitov, J. Sousa, A. A. Pais and E. Sparr, Biochimica et Biophysica Acta (BBA)-Biomembranes **1768** (11), 2647 (2007).

13.   J. W. Fluhr, P. Elsner, E. Berardesca and H. I. Maibach, *Bioengineering of the skin: water and the stratum corneum*. (CRC press, 2004).

14.   J. Sato, M. Yanai, T. Hirao and M. Denda, Arch Dermatol Res **292** (8), 412 (2000).

15.   M. Egawa, T. Hirao and M. Takahashi, Acta Derm-Venereol **87** (1), 4 (2007).

16.   J. M. Crowther, A. Sieg, P. Blenkiron, C. Marcott, P. J. Matts, R. Kaczvinsky and A. V. Rawlings, Brit J Dermatol **159** (3), 567 (2008).

17.   M. Egawa and T. Kajikawa, Skin Research and Technology **15** (2), 242 (2009).

18.   H. Loth, Int J Pharm **68** (1-3), 1 (1991).

19.   J. J. O. García and C. G. Treviño-Palacios, presented at the MEDICAL PHYSICS: Ninth Mexican Symposium on Medical Physics, 2006 (unpublished).

20.   M. J. Wan, X. Y. Su, Y. Zheng, Z. J. Gong, J. L. Yi, Y. Zhao, X. M. Guan and W. Lai, Int J Dermatol **54** (11), 1319 (2015).

21.   P. J. Caspers, G. W. Lucassen, E. A. Carter, H. A. Bruining and G. J. Puppels, J Invest Dermatol **116** (3), 434 (2001).

22.   K. Johnsen, M. Mahonen and P. Lunde, Scand Cardiovasc J **43** (3), 176 (2009).

23.   G. J. Zhang, A. Papillon, E. Ruvolo, P. R. Bargo and N. Kollias, Photonic Therapeutics and Diagnostics Vi **7548** (2010).

24.   K. Wichrowski, G. Sore and A. Khaiat, International journal of cosmetic science **17** (1), 1 (1995).

25.   H. Tagami, M. Ohi, K. Iwatsuki, Y. Kanamaru, M. Yamada and B. Ichijo, J Invest Dermatol **75** (6), 500 (1980).

26.   M. J. Adams, B. J. Briscoe and S. A. Johnson, Tribol Lett **26** (3), 239 (2007).

27.   S. Derler, R. M. Rossi and G. M. Rotaru, P I Mech Eng J-J Eng **229** (3), 285 (2015).

28.   F. D. Fleischli, F. Morf and C. Adlhart, Chimia **69** (3), 147 (2015).

29.   M. Boncheva, J. de Sterke, P. J. Caspers and G. J. Puppels, Exp Dermatol **18** (10), 870 (2009).

30.   C. Adlhart and W. Baschong, International Journal of Cosmetic Science **33** (6), 527 (2011).

31.   D. Shojo, H. Sugimori, S. Yamazaki and K. Kimura, High Perform Polym, 0954008315619998 (2015).

32.   H. Watanabe, T. Furuyama and K. Okazaki, Energy & Fuels **29** (8), 5415 (2015).

33.   E. Cznotka, S. Jeschke, S. Schmohl, P. Johansson and H.-D. Wiemhöfer, Journal of Coatings Technology and Research, 1.

34.   M. Schüttel, Master thesis, Zurich University of Applied Sciences, 2013.

35.   M. Egawa and H. Tagami, Brit J Dermatol **158** (2), 251 (2008).

36.   N. J. Everall, Appl Spectrosc **54** (10), 1515 (2000).

37.   L. Greenspan, Journal of research of the national bureau of standards **81** (1), 89 (1977).

38.   A. Wexler and S. Hasegawa, Journal of Research of the National Bureau of Standards **53** (1), 19 (1954).

39.   D. C. Swartzendruber, P. W. Wertz, K. C. Madison and D. T. Downing, J Invest Dermatol **88** (6), 709 (1987).

40.   N. Nakagawa, M. Matsumoto and S. Sakai, Skin Research and Technology **16** (2), 137 (2010).

41.   A. C. Park and C. B. Baddiel, J Soc Cosmet Chem **23** (1), 3 (1972).

42.   A. C. Park and C. B. Baddiel, J Soc Cosmet Chem **23** (1), 13 (1972).

43.   J. van Kuilenburg, M. A. Masen and E. van der Heide, P I Mech Eng J-J Eng **227** (J4), 349 (2013).

44.   M. Geerligs, Technical University Eindhoven, 2009.

45.   H. Arimoto and M. Egawa, Skin Research and Technology **21** (1), 94 (2015).

46.   S. Bielfeldt, V. Schoder, U. Ely, A. Van Der Pol, J. De Sterke and K. P. Wilhelm, *Assessment of human stratum corneum thickness and its barrier properties by in‑vivo confocal Raman spectroscopy*. (2009).

47.   P. M. Elias and K. R. Feingold, *Skin barrier*. (CRC Press, 2005).

48.   P. M. Elias, Semin Immunopathol **29** (1), 3 (2007).

49.   M. D. A. van Logtestijn, E. Dominguez-Huttinger, G. N. Stamatas and R. J. Tanaka, Plos One **10** (2) (2015).

50.   M. D. van Logtestijn, E. Domínguez-Hüttinger, G. N. Stamatas and R. J. Tanaka, Plos One **10** (2), e0117292 (2015).

51.   X. Li, R. Johnson and G. B. Kasting, J Pharm Sci-Us **105** (3), 1141 (2016).

52.   J. A. Bouwstra, A. de Graaff, G. S. Gooris, J. Nijsse, J. W. Wiechers and A. C. van Aelst, J Invest Dermatol **120** (5), 750 (2003).

53.   A. Schatzlein and G. Cevc, Brit J Dermatol **138** (4), 583 (1998).

54.   O. Simonetti, A. J. Hoogstraate, W. Bialik, J. A. Kempenaar, A. H. G. J. Schrijvers, H. E. Bodde and M. Ponec, Arch Dermatol Res **287** (5), 465 (1995).

55. R. G. vanderMolen, F. Spies, J. M. vantNoordende, E. Boelsma, A. M. Mommaas and H. K. Koerten, Arch Dermatol Res **289** (9), 514 (1997).

56. W. M. Haynes, *CRC handbook of chemistry and physics*. (CRC press, 2014).

57. O.Vaisala, *Humidity Conversion Formulas*. (Helsinki, 2013).

58. N. A. Lange, G. M. Forker and R. S. Burington, (1939).

59. H. A. Benson, Current drug delivery **2** (1), 23 (2005).

60. C. K. Field and M. D. Kerstein, The American journal of surgery **167** (1), S2 (1994).

61. F. Seyfarth, S. Schliemann, D. Antonov and P. Elsner, Clin Dermatol **29** (1), 31 (2011).

62. L. Baumann, The Journal of pathology **211** (2), 241 (2007).

63. L. C. Gerhardt, N. Mattle, G. Schrade, N. Spencer and S. Derler, Skin Research and Technology **14** (1), 77 (2008).